High-performance Ge p-i-n photodetector on Si substrate*

CHEN Li-qun (陈荔群)[1], HUANG Xiang-ying (黄祥英)[1], LI Min (李敏)[1], HUANG Yan-hua (黄燕华)[1], WANG Yue-yun (王月云)[1], YAN Guang-ming (严光明)[2], and LI Cheng (李成)[2]**

1. Chengyi College, Jimei University, Xiamen 361021, China

2. Semiconductor Photonics Research Center, Department of Physics, Xiamen University, Xiamen 361005, China

(Received 10 March 2015)

©Tianjin University of Technology and Springer-Verlag Berlin Heidelberg 2015

High-performance and tensile-strained germanium (Ge) p-i-n photodetector is demonstrated on Si substrate. The epitaxial Ge layers were prepared in an ultrahigh vacuum chemical vapor deposition (UHV-CVD) system using low temperature Ge buffer technique. The devices were fabricated by in situ doping and using Si as passivation layer between Ge and metal, which can improve the ohmic contact and realize the high doping. The results show that the dark current of the photodetector with diameter of 24 μm is about 2.5×10^{-7} μA at the bias voltage of –1 V, and the optical responsivity is 0.1 A/W at wavelength of 1.55 μm. The 3 dB bandwidth (BW) of 4 GHz is obtained for the photodetector with diameter of 24 μm at reverse bias voltage of 1 V. The long diffusion time of minority carrier in n-type Ge and the large contact resistance in metal/Ge contacts both affect the performance of Ge photodetectors.

Document code: A **Article ID:** 1673-1905(2015)03-0195-4

DOI 10.1007/s11801-015-5044-8

Si microphotonics has emerged as a promising technology to break through the interconnect bottlenecks in telecommunications and on-chip interconnects[1,2]. There is an increasing demand for complementary metal oxide semiconductor (CMOS) compatible low-cost, high-speed optical receivers. Epitaxial growth of germanium (Ge) on Si is promising for applications in the field due to its high absorption coefficient in the wavelength range of 1.3–1.55 μm for low-cost monolithic transceivers used in optical communications. Despite the large lattice mismatch (about 4.2%) between Ge and Si, several groups reported the epitaxial grown of Ge films on Si with electronic properties suitable for photodetectors. Linearly graded buffer layers[3], low temperature buffers[4,5] and thermal annealing[6] were employed to deposit Ge epilayers with low dislocation density. These methods are focused on bulk heteroepitaxial growth on Si. However, optimizing the device structure is also a promising approach for the monolithic integration of Ge optoelectronics on Si. Vivien et al[7,8] have observed Ge p-i-n photodetectors selectively grown at the end of Si waveguides, and a very high optical bandwidth (BW) up to 120 GHz and an optical responsivity of 0.8 A/W at 1 550 nm were measured. Park et al[9] reported Ge p-i-n photodiodes in which an i-Si layer was inserted between Ge and top Si layer to reduce the electric field in Ge layer, which had a low dark current density of 10 mA/cm^2 at –1 V without post-growth annealing.

With the latter technique, normal incidence p-i-n photodiodes were demonstrated with optical responsivity as high as 1 A/W at 1.55 μm (external quantum efficiency of 80%)[10]. The dark current density can reach 0.15 mA/cm^2 at reverse bias voltage of 1 V[11]. A large bandwidth of 49 GHz was recently achieved in normal incidence p-i-n diodes, which was realized by Ge grown on Si using molecular beam epitaxy[12]. However, the high dark current density and non-ohmic contact between Ge and metal are also common problems. In this paper, we demonstrate a 0.16% tensile strained Ge p-i-n photodetector integrated on a Si substrate using low- temperature Ge buffer layer technique. The in situ doping technology and using Si as passivation layer between n+ Ge and metal can make the ohmic contact better and improve the doping concentration. The devices are characterized in terms of dark current, optical responsivity and 3 dB bandwidth in the near infrared (NIR) region.

The schematic cross section of the detector is shown in Fig.1(a). Ge was epitaxially grown on an n-type (001) Si wafer with diameter of 10 cm by ultrahigh vacuum chemical vapor deposition (UHV-CVD) with a base pressure lower than 10^{-7} Pa. After standard Radio Corporation of America etching and thermal cleaning of Si substrate at 900 °C for 30 min, an Si buffer layer was grown at 650 °C for 30 min. In order to minimize the dislocation associated with the large lattice mismatch, firstly, a thin relaxed low-temperature Ge buffer with

* This work has been supported by the National Natural Science Foundation of China (Nos.61474094 and 61176092).

** E-mail: clq2113@163.com

thickness of 90 nm was grown at 330 °C followed by a high temperature growth at 600 °C to deposit 300 nm-thick Ge on Si. Then, a 150 nm-thick Ge layer, which was highly doped in situ with a B_2H_6 concentration of 1.5×10^{19} cm^{-3}, served as a p+ buried layer. In the next growth step, a fully strain relaxed 430 nm-thick intrinsic region was deposited with an abrupt transition of the doping level from 10^{19} cm^{-3} to the order of 10^{16} cm^{-3}. The in situ doping concentration of PH_3 was sharply increased to 2.5×10^{18} cm^{-3} in the following 300 nm-thick n+ Ge layer. Finally, a 2 nm-thick strained Si cap layer with a PH_3 doping concentration of 10^{20} cm^{-3} was used for the top ohmic contract.

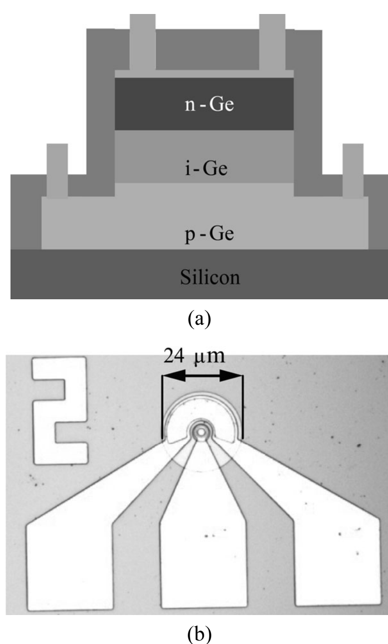

Fig.1 (a) Schematic cross section and (b) electrode structure of the 24 μm-diameter Ge p-i-n photodetector

The preparation process of device started with the formation of the active region in inductively coupled plasma (ICP) etcher. The etching depth must be thoroughly controlled to achieve a maximum remaining thickness of the p+ buried layer, which is essential for a small series resistance. In the second ICP etching step, the mesa of the n+ buried layer was patterned. Al was used as the metal contact by *e*-beam evaporation, and SiO_2 was used to insulate and passivate the devices by plasma-enhanced chemical vapor deposition on the sidewall to reduce the surface leakage current. No antireflection coating was deposited on the device. The micrograph of the photodetector with a 24 μm-diameter top mesa is shown in Fig.1(b). The strain status and the crystal quality of Ge were evaluated by double crystal X-ray diffraction (XRD) measurement (Bede, D1 system) using a Cu $K_{\alpha1}$ (λ=0.154 06 nm) X-ray source. The dopant distribution in the sample was measured by secondary ion mass spectrometry (SIMS). The current-voltage characteristics of the devices were measured with an Agilent B1500A semiconductor parameter analyzer at room temperature.

The in situ doped phosphorus and boron depth profiles measured by SIMS in sample are illustrated in Fig.2. The abrupt depth profiles of impurity concentration at the interface between doped and intrinsic Ge layers and the p-i-n structure are clearly visible. Although the flows of the PH_3 and B_2H_6 are well matched in the in situ doping, the phosphorus concentration of 2.5×10^{18} cm^{-3} is lower than the boron concentration of 1.5×10^{19} cm^{-3} by about one order of magnitude. The larger diffusivity of phosphorus which is proportional to the square of phosphorus concentration causes the extracted phosphorus to diffuse into the intrinsic Ge layer during the in situ growth process[13]. As a result, lower phosphorus concentration of n+ Ge layer and smaller thickness of intrinsic Ge layer compared with predicted values are achieved.

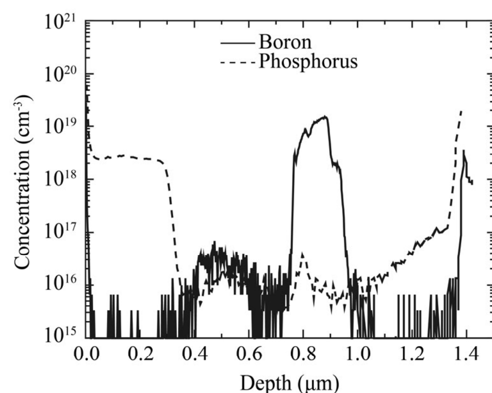

Fig.2 SIMS depth profiles of phosphorus and boron in n/p Ge layer

Fig.3 shows the typical measured XRD rocking curves of the Ge on Si substrate. With the rocking distance between Ge epilayer and Si layer, the tensile stain in Ge epilayer is evaluated to be about 0.16%, which should be due to the large thermal expansion coefficient difference between Ge and Si. The tensile strain in the grown Ge results in enhanced efficiency in the NIR region and shifts the absorption edge to longer wavelengths[14]. The full width at half maximum (FWHM) of Ge peak is about 236″. The narrower FWHM of Ge XRD peak suggests that the sample has good crystal quality.

The current-voltage characteristics in the dark and with illumination of the detector at 1.55 μm under forward and reverse bias voltages are shown in Fig.4, which shows better diode performance with a good rectification ratio of 10^4 at bias voltage of ±1 V. The dark current of photodetector with diameter of 24 μm is 2.5×10^{-7} A at reverse bias voltage of 1 V, corresponding to a current density of 55.3 mA/cm^2.

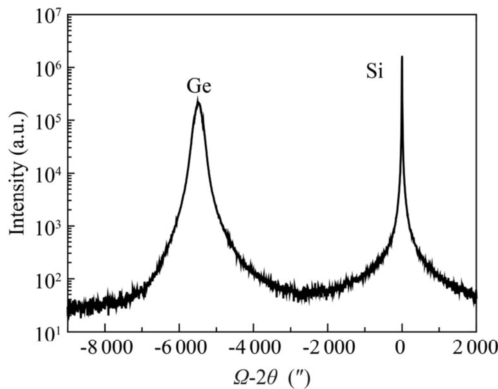

Fig.3 Measured XRD rocking curves of the sample with Ge on Si substrate

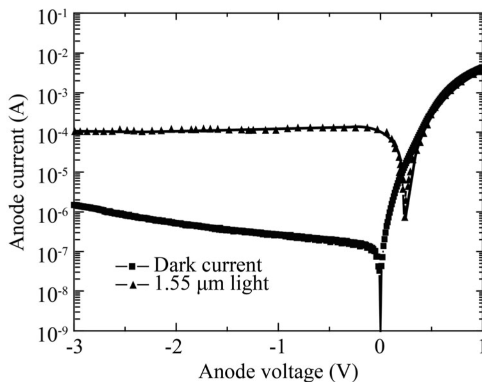

Fig.4 Measured dark current and photocurrent at 1.55 μm for 24 μm-diameter photodetector

The measurement of optical responsivity is performed with the use of a semiconductor analyzer, a probe station and a laser with wavelength of 1.55 μm. The light is coupled into the device completely with a single-mode fiber probe at incident optical power of 1 mW. The saturation of the photocurrent at 0 V bias voltage reveals that the photodetector configuration allows a complete photo-generated carrier collection without bias voltage. At a reverse bias voltage of 1 V, the optical responsivity of the p-i-n photodiode is 0.1 A/W at 1.55 μm, which is lower than the predicted value due to the higher contact resistance induced between low doped n+ Ge and metal and the parasitic capacitance in the photodiode.

The normalized frequency response of the 24 μm-diameter detector is measured by a distributed feedback laser at 1.55 μm. The frequency of modulation is swept over a bandwidth range of 80 MHz–10 GHz. The frequency responses at four bias voltages are shown in Fig.5. At the reverse bias voltages of 0 V and 1 V, the 3 dB bandwidths with mesa diameter of 24 μm are found to be 1.7 GHz and 4 GHz, respectively. At the reverse bias voltages of 3 V and 5 V, the bandwidths both decrease sharply. A destructive breakdown occurs when the reverse bias voltage is increased to 3 V. It is suggested that the fact that the thin and high doped n+ Ge layer is hardly achieved causes the minority hole to infuse into the intrinsic Ge layer, while large contact resistance induced between low doped n+ Ge and metal can reduce the performance of the device. On the other hand, the parasitic capacitance of the device increases when Ge material is used as virtual substrate due to its good conductivity, which reduces the high frequency performance of the photodetector[15].

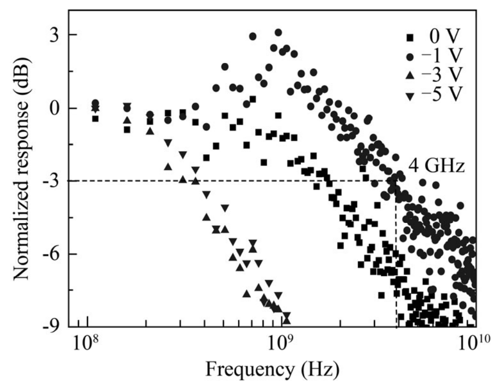

Fig.5 Normalized frequency responses of the 24 μm-diameter detector at different bias voltages

In conclusion, we demonstrate a 0.16% tensile strained normal incidence Ge p-i-n photodetector grown on Si substrate for monolithic integration using UHV-CVD. A low dark current of 2.5×10^{-7} A indicates the good Ge film quality at reverse bias voltage of 1 V. The optical responsivity of 0.1 A/W is achieved at 1.55 μm. The 3 dB bandwidths of the detector with diameter of 24 μm are 4 GHz and 1.7 GHz at bias voltages of –1 V and 0 V, respectively. The performance limitation of the photodetector should be attributed to the long diffusion time of minority carriers in n-type or p-type Ge and the large contact resistance induced by non-ohmic contact. The dark current density can be reduced by further improving the Ge epitaxial growth quality and fabrication. The bandwidth and the responsivity can be improved by using resonant cavity design while maintaining a thin intrinsic Ge layer for high-speed operation.

References

[1] Yu Cao, Jian-jun Zhang, Tian-wei Li, Zhen-hua Huang, Jun Ma, Xu Yang, Jian Ni, Xin-hua Geng and Ying Zhao, Journal of Optoelectronics·Laser **24**, 924 (2013). (in Chinese)

[2] Xiao-feng Shi, Xiang Cheng, Chao Chen, Ji-fang Li, Huang-ping Yan, Jiang-bing Pan and Cheng-cheng Fan, Journal of Optoelectronics·Laser **24**, 2086 (2013). (in Chinese)

[3] S. G. Thomas, S. Bharatan, R. E. Jones, R. Thoma, T. Zirkle, N. V. Edwards, R. Liu, X. D. Wang, Q. H. Xie, C. Rosenblad, J. Ramm, G. Isella and H. V. Känel, Journal of Electronic Materials **32**, 976 (2003).

[4] D. Choi, Y. Ge, J. S. Harris, J. Cagnon and S. Stemmer, Journal of Crystal Growth **310**, 4273 (2008).

[5] Y. Yamamoto, P. Zaumseil, T. Arguirov, M. Kittler and B. Tillack, Solid-State Electronics **60**, 2 (2011).
[6] Z. Liu, X. Hao, A. Ho-Baillie, C. Y. Tsao and M. A. Green, Thin Solid Films **574**, 99 (2015).
[7] L. Vivien, A. Polzer, D. Marris-Morini, J. Osmond, J. M. Hartmann, P. Crozat, E. Cassan, C. Kopp, H. Zimmermann and J. M. Fédéli, Optics Express **20**, 1096 (2012).
[8] L. Vivien, J. Osmond, J. M. Fédéli, D. Marris-Morini, P. Crozat, J. F. Damlencourt, E. Cassan, Y. Lecunff and S. Laval, Optics Express **17**, 6252 (2009).
[9] S. B. Park, S. Takita, Y. Ishikawa, J. Osaka and K. Wada, Chinese Optics Letters **7**, 286 (2009).
[10] S. B. Samavedam, M. T. Currie, T. A. Langdo and E. A. Fitzgerald, Applied Physics Letters **73**, 2125 (1998).
[11] S. Klinger, M. Berroth, M. Kaschel, M. Oehme and E. Kasper, IEEE Photonics Technology Letters **21**, 920 (2009).
[12] L. Chen, Y. Chen and C. Li, Optoelectronics Letters **10**, 213 (2014).
[13] S. Huang, C. Li, C. Chen, C. Wang, G. Yan, H. Lai and S. Chen, Applied Physics Letters **102**, 182102 (2013).
[14] Y. Huo, H. Lin, R. Chen, M. Makarova, Y. Rong, M. Li, T. I. Kamins, J. Vuckovic and J. S. Harris, Applied Physics Letters **98**, 011111 (2011).
[15] M. J. Deen and P. K. Basu, Silicon Photonics: Fundamentals and Devices, Manhattan: John Wiley & Sons, 2012.